JOURNAL OF COMPUTATIONAL PHYSICS 79, 184–199 (1988)

A Finite Element Code for the Simulation of One-Dimensional Vlasov Plasmas. I. Theory

S. I. ZAKI AND L. R. T. GARDNER

Department of Applied Mathematics and Computation, University of Wales, Bangor LL57 2UW, Wales

AND

T. J. M. BOYD

Department of Physics, University of Wales, Bangor LL57 2UW Wales

Received March 20, 1987; revised November 9, 1987

The Galerkin method is used to obtain a finite element solution to the Vlasov–Poisson equations over the two-dimensional (x, v) phase plane using bilinear element shape functions. A set of linear equations for updated values of the distribution function is obtained in which time-dependent and time-independent coefficients are separated to reduce the computation involved. The noise levels are low and the energy conservation good. The finite element approach offers certain advantages over alternative methods in applications to problems in plasma physics. In particular, the flexibility in using elements of different size allows problems in which regions of the plasma are characterized by often widely differing scale lengths to be treated efficiently.

1. INTRODUCTION

Numerical solutions of the Vlasov–Poisson system of equations to address problems in plasma physics have become commonplace since the early attempts by Dawson, Knorr, and others more than twenty years ago [1, 2]. Much attention has been given to finite difference methods [1–6] although waterbag models [7] have been widely used and with some success in view of their simplicity. In addition to these, transform [5, 6] and splitting [4] methods are important too, the latter in particular being both efficient and accurate for a range of problems.

Correspondingly, less work has been done using finite element methods [8] even though these might be expected to possess advantages over the others for certain classes of problems. In particular, one would expect low noise levels and accurate energy conservation and, by using elements of varying size, hope to deal efficiently with those problems such as plasma sheaths where, within the sheath, parameters vary rapidly compared with their behaviour in the bulk plasma. On top of these

0021-9991/88 $3.00

advantages the method is well suited to handling complicated boundaries which may arise in many practical applications.

With this in mind we have developed and tested a finite element approach to the numerical solution of the Vlasov–Poisson system. We integrate the Vlasov equation over phase space by a method that is second order in the time step. In Section 2 we present the normalized equation to be solved by the finite element method subject to the boundary conditions introduced in Section 3. A solution of Poisson's equation is given in Section 4 and this is later used in Section 6 to reduce the amount of computation required. The process of matrix assembly and storage is described in Section 5. Tests used to validate the numerical method outlined in this paper are detailed and discussed in Part II.

2. A Finite Element Solution to Vlasov's Equation

We begin by normalizing the single species one-dimensional Vlasov–Poisson system describing the physics of the plasma electrons

$$\frac{\partial f}{\partial t} + v\frac{\partial f}{\partial x} - \frac{e}{m}E\frac{\partial f}{\partial v} = 0$$

$$\frac{\partial E}{\partial x} = -4\pi\rho = 4\pi e\left[n_0 - \int_{-\infty}^{\infty} f\,dv\right],$$

where $f(x, v, t)$ is the electron distribution function, E is the electric field, and e and m are the electron charge and mass, respectively. The charge density in the plasma is $\rho(x, t)$ with electron density $N_e(x, t) = \int_{-\infty}^{\infty} f(x, v, t)\,dv$, whereas the ions provide a uniform neutralizing background with (average) number density n_0. The electron velocities v are selected from the Maxwellian distribution

$$f(v) = \frac{N_e(x)}{\sqrt{2\pi}V_e}\exp\left[-\frac{v^2}{2V_e^2}\right],$$

where $V_e = (\kappa T_e/m_e)^{1/2}$ is the electron thermal velocity and T_e is the electron temperature. The Debye length $\lambda_D = (\kappa T_e/4\pi n_0 e^2)^{1/2}$ and the plasma frequency $\omega_p = (4\pi n_0 e^2/m)^{1/2}$ have been used to scale the quantities appearing in the Vlasov–Poisson system so as to produce a non-dimensional set of equations. The spatial coordinate x has been normalized to λ_D, time t to $1/\omega_p$, velocities to $V_e(=\lambda_D\omega_p)$, the electric field E to $4\pi n_e\lambda_D$ and the distribution function to N/V_e. With this scaling the Vlasov–Poisson equations take the form

$$\frac{\partial f}{\partial t} + v\frac{\partial f}{\partial x} - E\frac{\partial f}{\partial v} = 0, \tag{1}$$

$$\frac{\partial E}{\partial x} = 1 - \int_{-\infty}^{\infty} f\,dv. \tag{2}$$

We shall assume that the one-dimensional system is of length L and will allow velocities in the range $|v| \leqslant v_{\max}$. The computational domain is therefore a rectangle in the x, v phase plane bounded by the lines $x=0$, $x=L$, $v=\pm v_{\max}$. This region is to be divided into rectangular finite elements [9] and the distribution function will be represented by

$$f^e(x, v, t) = N^e(x, v)\, \mathbf{f}^e(t) \tag{3}$$

for each element e, where $N^e(x, v)$ are the shape functions and $\mathbf{f}^e(t)$ the vector of nodal values for the element at time t. Substituting into (1) we obtain, for each element,

$$N^e \frac{\partial \mathbf{f}^e}{\partial t} + v \frac{\partial N^e}{\partial x} \mathbf{f}^e - E^e \frac{\partial N^e}{\partial v} \mathbf{f}^e. \tag{4}$$

Using Galerkin's method [9], with the shape function N^e as weight functions we find for each finite element of area R_e

$$K^e \frac{\partial \mathbf{f}^e}{\partial t} + L^e \mathbf{f}^e + M^e(t)\, \mathbf{f}^e, \tag{5}$$

where

$$K^e = \int_{R_e} N^{eT} N^e \, dx \, dv \tag{6}$$

$$L^e = \int_{R_e} N^{eT} \frac{\partial N^e}{\partial x} v \, dx \, dv \tag{7}$$

and

$$M^e(t) = -\int_{R_e} N^{eT} \frac{\partial N^e}{\partial v} E^e(t) \, dx \, dv. \tag{8}$$

The matrix M^e, however, depends on time through the electric field E^e and so must be recalculated at each time step. A way of avoiding much of this computation will be discussed in Section 6.

If all functions are expressed in normalized local coordinates (ξ, η) $0 \leqslant \xi, \eta \leqslant 1$ with origin at the lower left hand corner (x_0, v_0) of an element of sides (a, b) we have, for bilinear interpolation over the element shown in Fig. 1 the shape functions [9],

$$N^e(\xi, \eta) = [(1-\xi)(1-\eta), \eta(1-\xi), \xi(1-\eta), \xi\eta]. \tag{9}$$

The element matrices then become

$$K^e = ab \int_0^1 \int_0^1 N^{eT} N^e \, d\xi \, d\eta \tag{10}$$

$$L^e = b \int_0^1 \int_0^1 N^{eT} \frac{\partial N^e}{\partial \xi} (v_0 + b\eta) \, d\xi \, d\eta \tag{11}$$

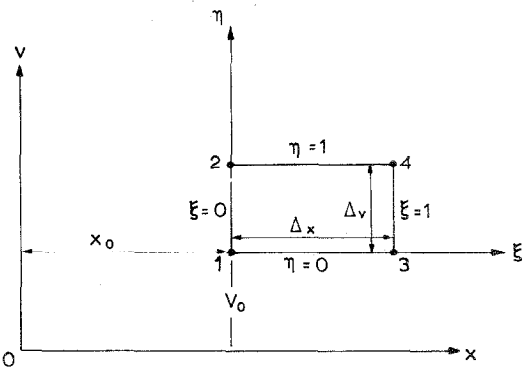

FIG. 1. Normalized co-ordinates for a rectangular finite element with nodal points 1, 2, 3, and 4 located at its corners.

and

$$M^e = -a \int_0^1 \int_0^1 N^{eT} \frac{\partial N^e}{\partial \eta} E^e \, d\xi \, d\eta. \tag{12}$$

After assembling the contributions for all elements we obtain the set of ordinary differential equations

$$K\dot{\mathbf{f}} + L\mathbf{f} + M(t)\mathbf{f} = 0, \tag{13}$$

where K, L, M have been constructed from the element matrices K^e, L^e, and M^e, respectively, and $\mathbf{f}$ is the total vector of nodal values for the distribution function.

We now linearly interpolate the distribution function between two adjacent time levels n and $n+1$ by writing the time variation of the distribution function as

$$f = [(1-\tau), \tau] \begin{bmatrix} \mathbf{f}^n \\ \mathbf{f}^{n+1} \end{bmatrix}, \tag{14}$$

where τ is related to the time t by $t = (n+\tau)\,\Delta t$ with $0 \leqslant \tau \leqslant 1$. Differentiating with respect to t we obtain

$$\dot{\mathbf{f}} = \frac{1}{\Delta t}(-1, 1) \begin{bmatrix} \mathbf{f}^n \\ \mathbf{f}^{n+1} \end{bmatrix}.$$

Hence (13) can be written as

$$\frac{K}{\Delta t}(\mathbf{f}^{n+1} - \mathbf{f}^n) + L[(1-\tau)\,\mathbf{f}^n + \tau \mathbf{f}^{n+1}] + M(\tau)[(1-\tau)\,\mathbf{f}^n + \tau \mathbf{f}^{n+1}] = 0. \tag{15}$$

The values of the parameter $\tau = 0$, $\frac{1}{2}$, and 1 correspond respectively to forward,

Crank–Nicholson, and backward difference shcemes. Setting $\tau = \frac{1}{2}$ and averaging f using

$$\mathbf{f}^{n+1/2} = \tfrac{1}{2}(\mathbf{f}^{n+1} + \mathbf{f}^{n}),$$

(15) takes the form

$$\frac{K}{\Delta t}(\mathbf{f}^{n+1} - \mathbf{f}^{n+1/2}) + \frac{K}{\Delta t}(\mathbf{f}^{n+1/2} - \mathbf{f}^{n}) + L\mathbf{f}^{n+1/2} + M^{n+1/2}\mathbf{f}^{n+1/2} = 0. \tag{16}$$

Instead of solving (16) as it stands, we solve an equivalent system of equations [9, 10]

$$\frac{K}{\Delta t}(\mathbf{f}^{n+1/2} - \mathbf{f}^{n}) + L\mathbf{f}^{n+1/2} = 0 \tag{17}$$

$$\frac{K}{\Delta t}(\mathbf{f}^{n+1} - \mathbf{f}^{n+1/2}) + M^{n+1/2}\mathbf{f}^{n+1/2} = 0. \tag{18}$$

The results of which will be an approximate solution for Eq. (16). Note that any solution which satisfies (17) and (18) will also satisfy (16), though the converse is not valid.

Equations (17) and (18) can be written in an implicit form for $\mathbf{f}^{n+1/2}$ and $\mathbf{f}^{n+1}$ as

$$\left[\frac{K}{\Delta t} + L\right]\mathbf{f}^{n+1/2} = \mathbf{f}^{n} \tag{19}$$

$$\frac{K}{\Delta t}\mathbf{f}^{n+1} = \left[-M^{n+1/2} + \frac{K}{\Delta t}\right]\mathbf{f}^{n+1/2}. \tag{20}$$

It is this system that we shall solve numerically. Various methods were tried, in the end we adopted Gauss–Seidel as being the most convenient.

The present paper thus solves the free streaming equation in x and the acceleration equation in v separately by implicit difference schemes. The method is related to the splitting scheme proposed by Cheng and Know [4], who solved the split equations by an interpolation approach in which no time differencing was used.

3. The Boundary Conditions

In many problems in plasma physics we wish to study phenomena over extensive regions of plasma. This is not usually possible numerically without making use of spatially periodic boundary conditions, and in the first instance we have followed this approach. In velocity space we must ensure that the region is wide enough to encompass all but a vanishingly small part of the distribution function at all times during the computer run. If this is satisfied we can set $f = 0$ at $v = \pm v_{\max}$.

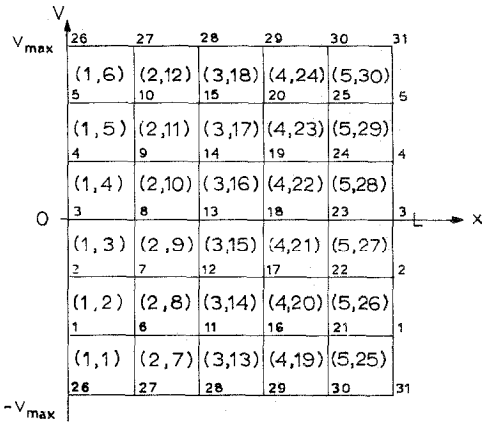

FIG. 2. An example of a phase plane divided into 30 elements with NHE = 5 and NVE = 6, under periodic boundary conditions in the x-direction.

The boundary conditions just discussed are enforced by an appropriate node numbering scheme. This is illustrated in Fig. 2 where the plane has been divided into 30 elements with 5 in the x direction and 6 in the v direction.

The periodic boundary condition is obtained by giving the nodes along the right-hand boundary the same numbers as those along the left. The $f = 0$ condition along the upper and lower boundaries is obtained by eliminating nodal variables f_{26} to f_{31} from (13) and also dropping Eqs. (26)–(32) from the set of 31 equations that (13) represents.

4. THE SOLUTION OF POISSON'S EQUATION

We now turn our attention to setting up a numerical solution to Poisson's equation in the form

$$\frac{\partial E}{\partial x} = 1 - \int_{-v_{max}}^{v_{max}} f(x, v, t)\, dv, \tag{2a}$$

where the electric field E is a function of x and t only.

Consider Fig. 2 and let us evaluate (2a) at a point x lying within $0 < x < a$, i.e., within the first column of elements. Suppose now instead of there being 5 internal nodes along the v direction we have M. Then this first column of elements and their nodal numbers is illustrated in Fig. 3.

In terms of (local) normalised coordinates (ξ, η) (2a) becomes, for a fixed point ξ lying within the first column of elements,

$$\frac{1}{a}\frac{\partial E}{\partial \xi} = 1 - b \sum_{\substack{\text{elements} \\ \text{in column 1}}} \int_0^1 N_i f_i^e \, d\eta. \tag{21}$$

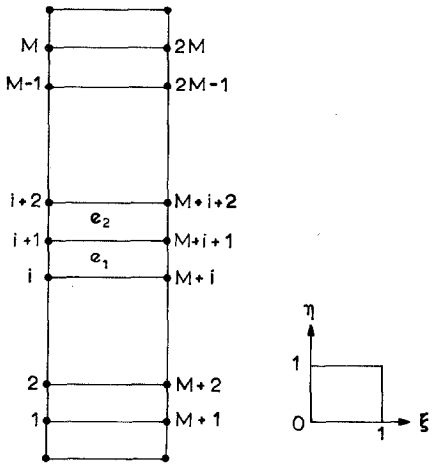

FIG. 3. The first column of elements from Fig. 2. Local normalized coords $(\xi\eta)$ vary $0 \leqslant \xi \leqslant 1$, $0 \leqslant \eta \leqslant 1$, over each element. The boundary nodes are shown but not numbered.

The integration with respect to η then involves only the first column of elements, shown in Fig. 3. These elements have nodes numbered 1 to $2M$.

We now examine the contribution of the nodal point $(i+1)$ to the integral. From Fig. 3 it is clear that the nodal point $(i+1)$ contributes to the integration over the two elements e_1 and e_2 in the following manner: over the element $e_1(1-\xi)[\frac{1}{2}f^e_{i+1}]$ and over the element $e_2(1-\xi)[1-\frac{1}{2}]f^e_{i+1}$. So the total contribution of the nodal value $(i+1)$ to the integral is $(1-\xi)f^e_{i+1}$. The nodal value $(M+i+1)$ contributes to the integral in Eq. (21) as follows: $\frac{1}{2}\xi f^e_{M+i+1}$ over the element e_1 and $\xi[1-\frac{1}{2}]f^e_{M+i+1}$ over the element e_2, so that the contribution of node $(M+i+1)$ in the η direction is ξf^e_{M+i+1}.

Now, since f_i is zero on $v = \pm v_{\max}$ only interior points contribute to the integral. Hence we can write the integral in (21) in the single form

$$\sum_{\substack{\text{all elements}\\ \text{in column 1}}} \int_0^1 N\mathbf{f}^e \, d\eta = (1-\xi) \sum_{i=2}^{M-1} f_i + \xi \sum_{M+2}^{2M-1} f_i \tag{22}$$

and then Poisson's equation takes the form

$$\frac{1}{a}\frac{\partial E}{\partial \xi} = 1 - b\left[(1-\xi) \sum_{i=2}^{M-1} f_i + \xi \sum_{i=M+2}^{2M-1} f_i\right]. \tag{23}$$

Note that $\partial E/\partial \xi$ is linear in ξ and independent of η and remember that it is valid, only, over a single strip of finite elements—the first column in Fig. 2.

Let us now integrate in the ξ (or x) direction to determine E. Integration over strip 1 leads to

$$\frac{1}{a}[E(\xi)-E(0)]=\xi-b\left[\left[\xi-\frac{1}{2}\xi^2\right]\sum_{i=2}^{M-1}f_i+\frac{1}{2}\xi^2\sum_{i=M+2}^{2M-1}f_i\right] \tag{24}$$

or simply at the right hand, where $\xi=1$,

$$\frac{1}{a}[E(1)-E(0)]=1-b\left[\frac{1}{2}\sum_{i=2}^{M-1}f_i+\frac{1}{2}\sum_{i=M+2}^{2M-1}f_i\right]. \tag{25}$$

Similarly, rewriting (23) for the 2nd strip and integrating with respect to ξ gives

$$\frac{1}{a}[E(\xi)-E(1)]=\xi-b\left[\left[\xi-\frac{1}{2}\xi^2\right]\sum_{i=M+2}^{2M-1}f_i+\frac{1}{2}\xi^2\sum_{i=2M+2}^{3M-1}f_i\right]$$

or at the right-hand node where $\xi=1$ again

$$\frac{1}{a}[E(2)-E(1)]=1-b\left[\frac{1}{2}\sum_{i=M+2}^{2M-1}f_i+\frac{1}{2}\sum_{i=2M+2}^{3M-1}f_i\right].$$

Using (25) this gives

$$\frac{1}{a}[E(2)-E(0)]=2-b\left[\frac{1}{2}\sum_{i=2}^{M-1}f_i+\sum_{i=M+2}^{2M-1}f_i+\frac{1}{2}\sum_{2M+2}^{3M-1}f_i\right]. \tag{26}$$

Introducing the notation

$$F(I)=\sum_{i=I^*M-2}^{(I+1)M-1}f_i, \tag{27}$$

we have

$$\begin{aligned}
&\frac{1}{a}(E(1)-E(0))=1-b\left[\frac{1}{2}F(0)+\frac{1}{2}F(1)\right]\\
&\frac{1}{a}(E(2)-E(0))=2-b\left[\frac{1}{2}F(0)+F(1)+\frac{1}{2}F(2)\right] \qquad (28)\\
&\qquad\vdots\\
&\frac{1}{a}(E(n-1)-E(0))=(n-1)-b\left[\frac{1}{2}F(0)+F(1)+\cdots+F(n-2)+\frac{1}{2}F(n-1)\right].
\end{aligned}$$

Values of the electric field at grid points lying along the x-direction are determined once the value of $E(0)$ is known. We shall use the condition commonly

used in periodic electrostatic codes, that the average value of the electric field is zero. Hence summing over all grid points we have

$$\frac{1}{a}\left[\sum_{i=0}^{n-1} E(i) - nE(0)\right] = \sum_{i=1}^{n-1} i - b\left[\frac{n-1}{2}(F(0)+F(1)) + \frac{n-2}{2}(F(1)+F(2)) + \cdots \frac{1}{2}(F(n-2)+F(n-1))\right], \tag{29}$$

where n the total number of nodes in the x-direction.

We now require that the average value of the electric field be zero, that is $\sum_{i=0}^{n-1} E(i) = 0$ which can be used in (29) to determine $E(0)$ through

$$E(0) = \frac{1}{M}\left\{\sum_{i=0}^{n-1} E(i) - a\sum_{i=1}^{n-1} i + ab\left[\frac{n-1}{2}(F(0)+F(1)) + \frac{n-2}{2}(F(1)+F(2)) + \cdots + \frac{1}{2}(F(n-2)+F(n-1))\right]\right\} \tag{30}$$

in terms of the known quantities $F(I)$.

Now that $E(0)$ has been determined, we can evaluate the nodal values of the electric field, that is $E(1)$, $E(2)$, ..., $E(n-1)$, by substituting $E(0)$ into (28). From (24) we can see that over each element the electric field varies quadratically in the x-direction. Therefore, if we seek to express this in finite element form we have three unknown parameters in each trial function which we will have to evaluate using three nodal variables for each element. For the rectangular element and an electric field which varies only in the x-direction we proceed by taking the electric field to be of the form

$$E^e(\xi) = \alpha_1 + \alpha_2\xi + \alpha_3\xi^2.$$

It is convenient to replace the constants α_1, α_2, α_3 by nodal values of the electric field. Taking equally spaced nodes in the element at $\xi = 0, \frac{1}{2}, 1$ so that the nodal values of the electric field are E_0, $E_{1/2}$, E_1 produces a vector of nodal parameters

$$\boldsymbol{\delta}^e = \begin{pmatrix} E_0 \\ E_{1/2} \\ E_1 \end{pmatrix}$$

in terms of which the electric field is

$$E^e(\xi) = [1 - 3\xi + 2\xi^2,\ 4\xi - 4\xi^2,\ -\xi + 2\xi^2] \begin{pmatrix} E_0 \\ E_{1/2} \\ E_1 \end{pmatrix}. \tag{31}$$

We need, therefore, to know the values of the electric field at the points $\xi = 0$, $\xi = \frac{1}{2}$, $\xi = 1$ over each strip. For the first strip $E_0 = E(0)$, $E_1 = E(1)$ have already been determined in (30) and (28) and we can use (24) to evaluate the third nodal parameter $E_{1/2} = E(\frac{1}{2})$ as

$$E(\tfrac{1}{2}) = E(0) + a\left[\frac{1}{2} - \frac{b}{8}(3F(0) + F(1))\right].$$

An extension of that equation enables us to determined the field at the midpoint of each strip as

$$E\left[\frac{2i+1}{2}\right] = E(i) + a\left[\frac{1}{2} - \frac{b}{8}(3F(i) + F(i+1))\right], \qquad i = 0, 1, ..., n. \tag{32}$$

An expression for the distribution of the electric field over each element, of the form (31), has therefore been set up. This will be used later to enable us to reduce the amount of computation required at each time step.

5. The Assembly Process

In this section we discuss how the differential equations governing the whole system are constructed from the element (5). We also describe devices by means of which core storage requirements may be reduced. Note that since the elements are laid out and numbered systematically (see Fig. 2), we do not in fact need to store the values l, m, n, and k for each and every element because there is a relationship between these four values. If $NV+1$ is the number of nodes in the v direction, then for an interior element with nodal number l at its lower left-hand corner, the other three nodal numbers are given by

$$m = l + 1$$
$$n = l + (NV - 1)$$
$$k = n + 1.$$

Thus, once the value of l is prescribed, the values of m, n, and k are also known.

In the assembly process, the elements

$$K^e\dot{\mathbf{f}}^e + L^e\mathbf{f}^e + M\mathbf{f}^e,$$

where K^e, L_e, and M^e are 4×4 matrices and $\mathbf{f}^e$ is the 4×1 vector of nodal parameters, are combined together to give the differential equations which govern the whole system, viz,

$$K\dot{\mathbf{f}} + L\mathbf{f} + M\mathbf{f} = 0,$$

where **f** is the $N \times 1$ vector of all nodal parameters and K, L, and M are $N \times N$ matrices. Suppose the rectangular element has nodes numbered (l, m, n, k), then the typical element matrix S^e will have the form

$$\begin{pmatrix} S^e(l,l) & S^e(l,m) & S^e(l,n) & S^e(l,k) \\ S^e(ml) & \cdots & & \\ \cdots & & & \end{pmatrix}.$$

Here S^e is used to represent the element matrices K^e, L^e, or M^e. Now if S represents the assembled matrix for the whole structure then the relation between S and S^e will be

$$S(i, j) = \sum S^e(i, j),$$

where the sum is over all elements and S here represents the assembled form of K, L, or M.

In Fig. 4, we illustrate the assembled matrix S and show in boxes the contributions made to it by the typical finite element (3, 16) (see Fig. 1). When contributions from all the elements are included, S takes the form shown in Fig. 4a, where the only non-zero matrix elements are shown as stars. One can see that the

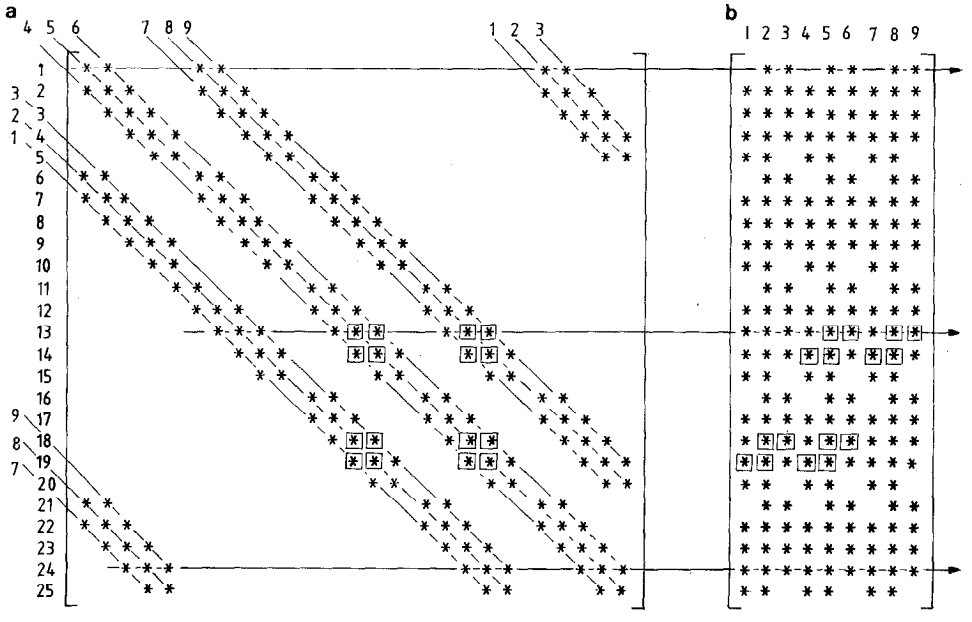

FIG. 4. Position of the nonzero entries in the assembled matrix and, the associated block matrix Fig. 4a for a periodic plasma in the x-direction with a phase plane divided into 30 elements with $NHE = 5$ and $NVE = 6$.

matrix S has some structure imposed on it by the node numbering scheme and the boundary conditions.

If the three matrices K, L, and M having this form are stored in memory without modifications, many unnecessary zero elements are included. For example, the matrix S in Fig. 4a includes 625 elements, of which 430 are zero. Storage can, however, be reduced if we are able to identify the indices of non-zero matrix elements, and so omit from core most of the zero matrix elements. The way this may be accomplished is shown schematically in Fig. 4b. The diagonal lines shown in Fig. 4a are rotated until they are vertical and the matrix elements translated into the appropriate locations SB in Fig. 4b. The original relative vertical positioning of the matrix elments is retained.

It is seen that the square stiffness matrix S of size $(N \times N)$ can in fact be replaced by a rectangular array SB of size $N \times 9$ thus saving an area of memory of size $N \times (N-9) \times 3$, since S represents the 3 matrices K, L, and M.

6. Derivation of a Time–Independent Matrix M

The matrix M in (13) is of course a function of time since it includes $E(t)$. This implies that M^e must be recalculated and M reassembled at each time step and this is clearly undesirable.

Ways of removing the time-dependent part of the electric field from the integrand have been devised. This was achieved by using an expression for the electric field over a finite element in terms of its nodal values

$$E^e = (1 - 3\xi + 2\xi^2,\ 4\xi - 4\xi^2,\ -\xi + 2\xi^2) \begin{pmatrix} E_0 \\ E_{1/2} \\ E_1 \end{pmatrix} = E\mathbf{e} = \mathbf{e}^T E^T, \tag{33}$$

where

$$E = (1 - 3\xi + 2\xi^2,\ 4\xi - 4\xi^2,\ -\xi + 2\xi^2) \tag{34}$$

and

$$e = \begin{pmatrix} E_0 \\ E_{1/2} \\ E_1 \end{pmatrix} \tag{35}$$

is the vector which contains the nodal values of the electric field for the element of interest and so it is independent of ξ and η and can be taken outside any integration. So, using (33) in (12), we have for the element (ij) of matrix M^e

$$M^e_{ij} = -ae^T \int_0^1 \int_0^1 E^T N_i^{eT} \frac{\partial N_j^e}{\partial \eta}\, d\xi\, d\eta = -ae^T M^{e*}_{ij}, \tag{36}$$

where

$$M_{ij}^{e*} = \int_0^1 \int_0^1 E^T N_i^{eT} \frac{\partial N_j^e}{\partial \eta} \, d\xi \, d\eta \tag{37}$$

is itself a (3×1) matrix, independent of time. From (36) it is clear that each element of the matrix M^e has become the product of two matrices, one dependent on time, namely e, and the other M_{ij}^{e*}, time independent. Now it is of interest to write the (12×4) matrix M^e as a combined form (as we did with its elements) such that the assembling process can be carried out independently of the time level:

$$M^{e*} = \iint d\xi \, d\eta \begin{bmatrix} E_1 N_1^{eT} \dfrac{\partial N_1^e}{\partial \eta} & E_1 N_1^{eT} \dfrac{\partial N_2^e}{\partial \eta} & E_1 N_1^{eT} \dfrac{\partial N_3^e}{\partial \eta} & E_1 N_1^{eT} \dfrac{\partial N_4^{eT}}{\partial \eta} \\ E_2 N_1^{eT} \dfrac{\partial N_1^e}{\partial \eta} & — & — & E_2 N_1^{eT} \dfrac{\partial N_4^{eT}}{\partial \eta} \\ E_3 N_1^{eT} \dfrac{\partial N_1^e}{\partial \eta} & — & — & E_3 N_1^{eT} \dfrac{\partial N_4^e}{\partial \eta} \\ E_1 N_2^{eT} \dfrac{\partial N_1^e}{\partial \eta} & E_1 N_2^{eT} \dfrac{\partial N_2^e}{\partial \eta} & E_1 N_2^{eT} \dfrac{\partial N_3^e}{\partial \eta} & E_1 N_2^{eT} \dfrac{\partial N_4^e}{\partial \eta} \\ E_2 N_2^{eT} \dfrac{\partial N_1^e}{\partial \eta} & — & — & E_2 N_2^{eT} \dfrac{\partial N_4^e}{\partial \eta} \\ E_3 N_2^{eT} \dfrac{\partial N_1^e}{\partial \eta} & — & — & E_3 N_2^{eT} \dfrac{\partial N_4^e}{\partial \eta} \\ \vdots & \vdots & \vdots & \vdots \\ E_3 N_4^{eT} \dfrac{\partial N_1^e}{\partial \eta} & E_3 N_4^{eT} \dfrac{\partial N_2^e}{\partial \eta} & E_3 \dfrac{\partial N_4^e}{\partial \eta} \dfrac{\partial N_3^e}{\partial \eta} & E_3 N_4^{eT} \dfrac{\partial N_4^e}{\partial \eta} \end{bmatrix}. \tag{38}$$

For compatibility, we define e^* as

$$e^* = \begin{pmatrix} E_0 & E_{1/2} & E_1 & 0 & 0 & 0 & 0 & 0 & 0 & 0 & 0 & 0 \\ 0 & 0 & 0 & E_0 & E_{1/2} & E_1 & 0 & 0 & 0 & 0 & 0 & 0 \\ 0 & 0 & 0 & 0 & 0 & 0 & E_0 & E_{1/2} & E_1 & 0 & 0 & 0 \\ 0 & 0 & 0 & 0 & 0 & 0 & 0 & 0 & 0 & E_0 & E_{1/2} & E_1 \end{pmatrix}, \tag{39}$$

so that e^* is of size (4×12).

From (36), (38), and (39) it is clear that

$$M^e \equiv -a(e^T M_{ij}^{e*})_{i,j=1,\ldots,4} \equiv -ae^* M^{e*}, \tag{40}$$

where

$$[e^T M_{ij}^{e*}]_{i,j=1,\ldots,4} \equiv \begin{pmatrix} e^T M_{11}^{e*} & \cdots & e^T M_{14}^{e*} \\ \vdots & & \\ e^T M_{41}^{e*} & & e^T M_{44}^{e*} \end{pmatrix} \tag{41}$$

and so M^e is a product of two matrices one of which e^* is time dependent and M^{e^*} which is time independent. Now, since the matrix M^{e^*} is independent of time and also independent of the nodal values for the electric field, M^{e^*} will be the same for all the elements in the phase space for all time.

Before proceeding further, let us study the relation between the element matrices and the nodal values for the electric field. Consider the example shown in Fig. 2, and notice that if we take the values of the electric field at the nodal points along the x-axis to be $E_0, E_1, E_2, \ldots, E_n$, then the element matrices on the first strip (that is, the elements (1, 1), (1, 2), ..., (1, NV)), where NV is the number of nodes in the v direction, depend upon the nodal values E_0, $E_{1/2}$, and E_1 of the electric field, while the element matrices for the elements on the second strip (that is (2, 7), (2, 8), ..., (2, $2NV$)) depend upon the nodal values E_1, $E_{3/2}$, and E_2, and so on for the rest of the strips.

The contributions to the nodal point "14," for example (see Fig. 2), depend on those contributions from the surrounding elements, that is, the elements (2, 10), (2, 11), (3, 16), and (3, 17). Two of these four elements lie on strip two, that is, the elements (2, 10) and (2, 11), while the others (3, 16) and (3, 17) lie on the third strip. Consequently we cannot simply sum the contributions to the nodal point "14" as in our previous assembly procedure, but have to find a new way of storing the contributions and at the same time be able to combine them with the appropriate nodal value of the electric field. To do so, let us assume that the rectangular element e has the nodal numbers (l, m, n, k) and rewrite the matrix M^{e^*} in the compact form

$$M^{e^*} = \begin{pmatrix} M^{e^*}_{l,l} & M^{e^*}_{l,m} & M^{e^*}_{l,n} & M^{e^*}_{l,k} \\ M^{e^*}_{m,l} & M^{e^*}_{m,m} & M^{e^*}_{m,n} & M^{e^*}_{m,k} \\ M^{e^*}_{n,l} & M^{e^*}_{n,m} & M^{e^*}_{n,n} & M^{e^*}_{n,k} \\ M^{e^*}_{k,l} & M^{e^*}_{k,m} & M^{e^*}_{k,n} & M^{e^*}_{k,k} \end{pmatrix}, \tag{42}$$

where the elements are themselves 3×1 column vectors

$$M^{e^*}_{i,j} = \begin{pmatrix} M^{e^{**}}_{i,j,1} \\ M^{e^{**}}_{i,j,2} \\ M^{e^{**}}_{i,j,3} \end{pmatrix}, \qquad i, j = l, m, n, k, \tag{43}$$

the elements of which are given by

$$M^{e^{**}}_{ijp} = \int_0^1 \int_0^1 E_p N^e_i \frac{\partial N^e_j}{\partial \eta} \, d\xi \, d\eta, \qquad p = 1, 2, 3, \tag{44}$$

so that $M^{e^{**}}$ is a brick matrix of size $(4 \times 4 \times 3)$.

The element matrices $M^{e^{**}}_{ijp}$ are now assembled into the matrix M^* as

$$M^*_{i,j,P+2} = \sum_e M^{e^{**}}_{i,j,P}, \qquad i = l, m, n, k; \; j = l, m; \; P = 1, 2, 3; \tag{45}$$

$$M^*_{i,j,P} = \sum M^{e^{**}}_{i,j,P}, \qquad i = l, m, n, k; \; j = n, k; \; P = 1, 2, 3; \tag{46}$$

where l, m, n, and k are the nodal numbers of the rectangular element "e." M^* is a brick array of size $N \times N \times 5$, where N is the total number of nodes. The matrix M^* is independent of time and need be calculated only once. We now rearrange the nodal values of the electric field into a matrix of size $N \times 5$ which on multiplication by M^* produces the square matrix M. This matrix is

$$\varepsilon = \begin{pmatrix} E_{N-1} & E_{N-1/2} & E_0 & E_{1/2} & E_1 \\ E_0 & E_{1/2} & E_1 & E_{3/2} & E_2 \\ E_1 & E_{3/2} & E_2 & E_{5/2} & E_3 \\ \vdots & \vdots & \vdots & \vdots & \vdots \\ E_{N-3} & E_{N-5/2} & E_{N-2} & E_{N-1/2} & E_{N-1} \\ E_{N-2} & E_{N-3/2} & E_{N-1} & E_{N-1/2} & E_0 \end{pmatrix}. \tag{47}$$

Then

$$M_{ij} = \sum_{p=1}^{5} M^*_{ijp} \varepsilon(q, p), \tag{48}$$

where

$$q = 1, 2, ..., 2NX,$$
$$j = 1, 2, ..., N$$
$$i = (q-1)(NV-1)+1, ..., q(NV-1),$$

and NV, NX are the number of nodes in the v and x directions, respectively. We can easily reconstruct the time dependent matrix M_{ij} (13) by multiplying the time independent brick matrix M^*_{ijp} by the time dependent "matrix" of electric field values ε. The "matrix" ε is the only one that must now be recalculated at each time step and since ε depends only on the nodal values of the electric field this is simply and speedily accomplished.

To discuss the equality (48) and see what it means in real terms, suppose that q has the value 1; then, accordingly, i will take the values 1, 2, ..., $(NV-1)$, while j has the values 1, 2, 3, ..., N. These values for i and j represent the first band of the matrix M shown in Fig. 4a. Indeed these elements are the result of contributions due to those elements lying on the first column of Fig. 2, and the elements on the right-hand top corner of M are of these elements which lie on the last right-hand column of Fig. 2. Therefore, as we discussed before, these contributions depend mainly on the values $\varepsilon(1, P)$, $P = 1, 2, ..., 5$ of the electric field. If q has the value 2 then i takes the values $NV, ..., 2(NV-1)$, which represent the second band of the matrix M, Fig. 4a. As before, we notice that the elements on that band derive from contributions due to the elements of the first and second columns of Fig. 2. Therefore, these contributions depend mainly on the values $\varepsilon(2, P)$, $P = 1, 2, ..., 5$ of the electric field. Proceeding in the same way for values of q and i, the matrix M is recovered.

In part II we apply the finite element scheme for solving the Vlasov equation outlined in this paper to a range of test problems to provide a comprehensive check on the accuracy of the method.

REFERENCES

1. G. KNORR, *Naturforsch* **18A**, 1304 (1963).
2. T. P. ARMSTRONG, *Phys. Fluids* **10**, 1269 (1967).
3. J. DENAVIT AND W. L. KRUER, *Phys. Fluids* **8**, 1782 (1971).
4. C. Z. CHENG AND G. KNORR, *J. Comput. Phys.* **22**, 330 (1976).
5. A. J. KLIMAS, *J. Comput. Phys.* **50**, 270 (1982).
6. T. P. ARMSTRONG, R. HARDING, G. KNORR, AND D. MONTGOMERY, "Solution of the Vlasov equation by transform methods," *Methods in Computational Physics*, Vol. 9 (Academic Press, New York, 1970).
7. D. POTTER, *Computational Physics* (Wiley, New York, 1973).
8. V. ERZ, E. RÄUCHLE, AND K. WEIXELBAUM, in *Proceedings, 5th Intl. Conf. on Plasma Physics, Gothenberg, Sweden, 1982*, Vol. 1, p. 309.
9. O. C. ZIENKIEWICZ, *The Finite Element Method*, 3rd ed., (McGraw–Hill, New York, 1982).
10. A. R. MITCHELL AND D. F. GRIFFITHS, *The Finite Difference Method in Partial Differential Equations* (Wiley, New York, 1980).